



Contents lists available at ScienceDirect

Bioorganic & Medicinal Chemistry

journal homepage: www.elsevier.com/locate/bmc



Development of antiproliferative phenylmaleimides that activate the unfolded protein response

Ulrike Muus^a, Curtis Hose^b, Wei Yao^c, Teresa Kosakowska-Cholody^d, David Farnsworth^a, Marzena Dyba^e, George T. Lountos^f, David S. Waugh^f, Anne Monks^b, Terrence R. Burke Jr.^{a,*}, Christopher J. Michejda^{c,†}

^a Chemical Biology Laboratory, Molecular Discovery Program, NCI-Frederick, Frederick, MD 21702, USA

^b Screening Technologies Branch, SAIC-Frederick, Inc., Frederick, MD 21702, USA

^c Structural Biophysics Laboratory, Molecular Discovery Program, NCI-Frederick, Frederick, MD 21702, USA

^d Laboratory of Cell and Developmental Signaling, NCI-Frederick, Frederick, MD 21702, USA

^e Structural Biophysics Laboratory, SAIC-Frederick, Inc., NCI-Frederick, Frederick, MD 21702, USA

^f Macromolecular Crystallography Laboratory, NCI-Frederick, Frederick, MD 21702, USA

ARTICLE INFO

Article history:

Received 4 March 2010

Revised 19 April 2010

Accepted 20 April 2010

Available online 24 April 2010

This work is dedicated to the memory of Dr. Christopher J. Michejda

Keywords:

Cdc25

Antiproliferative

Unfolded protein response

Protein alkylation

ABSTRACT

The current paper presents the synthesis and evaluation of a series of maleimides that were designed to inhibit the Cdc25 phosphatase by alkylation of catalytically essential cysteine residues. Although in HepB3 cell culture assays the analogues did exhibit antiproliferative IC₅₀ values ranging from sub-micromolar to greater than 100 μM, inhibition of Cdc25 through cysteine alkylation could not be demonstrated. It was also found that analysis using fluorescence activated cell sorting (FACS) following treatment with the most potent analogue (**1t**) did not provide data consistent with inhibition at one specific point in the cell cycle, as would be expected if Cdc25A were inhibited. Further studies with a subset of analogues resulted in a correlation of antiproliferative potencies with activation of the unfolded protein response (UPR). The UPR is a regulatory pathway that temporarily suspends protein production when misfolding of proteins occurs within the endoplasmic reticulum (ER). In addition, ER chaperones that promote proper refolding become up-regulated. If cellular damage cannot be resolved by these mechanisms, then the UPR can initiate apoptosis. The current study indicates that these maleimide analogues lead to UPR activation, which is predictive of the selective antiproliferative activity of the series.

Published by Elsevier Ltd.

1. Introduction

Phenylmaleimides of type **1** (Fig. 1) have recently been reported to exhibit growth inhibition against liver cancer cell lines in vitro and antitumor activity in vivo in Fischer 344 rats carrying an orthotopic model of hepatocellular carcinoma.¹ The design of these compounds was originally based on benzoquinone Cdc25 phosphatase inhibitors, such as 2-(2-mercaptoethanol)-3-methyl-1,4-naphthoquinone (**3**) and 2,3-bis-[2-hydroxyethylsulfanyl]-1,4-naphthoquinone (**4**) (Fig. 1).^{2,3} Phosphatase inhibition by naphthoquinones has been shown to occur by alkylation of the enzyme's catalytic cysteine residue.⁴ The phenylmaleimides were designed to alkylate the phosphatase catalytic cysteine via a 1,4-Michael-type mechanism, but to be distinct from the naphthoquinones in not promoting oxidative recycling that can occur with the latter.⁵ As presented in our current report, we prepared a series of structurally diverse N-aryl and N-alkyl maleimides (**1** and **2**, respectively, Fig. 1) that

exhibit differential antiproliferative potencies in HEP3B cell growth assays. When we were unable to demonstrate the originally intended Michael acceptor-based inhibitory effects on Cdc25 phosphatases, we examined potential causes of antiproliferation not directly related to inhibition of Cdc25 phosphatases. We were able to show that the phenylmaleimides differentially activate unfolded protein response (UPR) pathways and that these latter actions of the phenylmaleimides could contribute to their overall antiproliferative profiles.

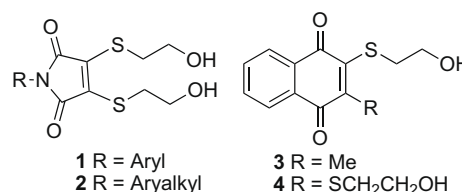
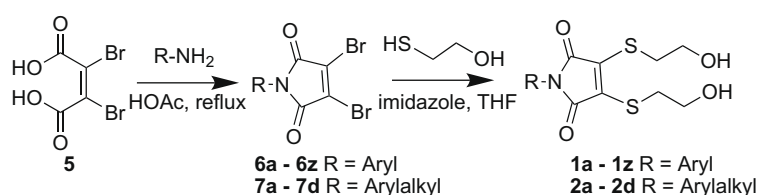


Figure 1. Structures of N-substituted maleimides (**1** and **2**) and benzoquinone Cdc25 phosphatase inhibitors (**3** and **4**).

* Corresponding author. Tel.: +1 301 846 5906; fax: +1 301 846 6033.

E-mail address: tburke@helix.nih.gov (T.R. Burke).

† Deceased.



Scheme 1. Synthesis of target maleimides with 'R' as defined in Tables 1 and 2.

2. Results and discussion

2.1. Synthesis

The synthesis of *N*-substituted maleimides **1a–1z** and **2a–2d** (Scheme 1) began by reacting 3,4-dibromomaleic acid (**5**) with the appropriate amines in refluxing acetic acid to give the corresponding 3,4-dibromomaleimides (**6a–6z** and **7a–7d**, respectively) in yields of 33–93% (Scheme 1). Treatment of the dibromo-intermediates with 2-mercaptoethanol in the presence of imidazole in tetrahydrofuran followed by silica gel flash chromatographic purification gave the desired final products (Scheme 1). In an alternate approach, *N*-substituted maleimides were brominated to yield a mixture of 3-bromo and 3,4-dibromo products.⁶ Reaction with mercaptoethanol as indicated above, gave the corresponding mono- and di-substituted adducts, which were subjected to chromatographic purification to provide the final products **1a–1z** and **2a–2d**.

2.2. Evaluation of growth inhibition

The antiproliferative effects (IC_{50} values defined as the concentration of inhibitor causing a 50% reduction of cell number relative to untreated controls) of **1a–1z** and **2a–2d** were determined using a HEP3B cell growth inhibition assay.¹ The naphthoquinone-based Cdc25 phosphatase inhibitors **3** and **4** were also included for comparison, since they had served as models in the original design of the maleimide series of compounds. With few exceptions (i.e., **1q**, **1r** and **1w**) the *N*-aryl-substituted maleimides (**1a–1z**, Table 1) and the *N*-arylalkyl-substituted maleimides (**2a–2d**, Table 2) were found to inhibit cell growth in a dose-dependent manner. The growth inhibition of **1b–1p**, which contained a variety of substituents at the phenyl 2-, 3- and 4-positions, were all highly uniform (IC_{50} values of between 4 and 10 μ M) and approximately one order of magnitude greater than the unsubstituted parent (**1a**, IC_{50} = 70 μ M). This data indicated that most of the aryl substituents enhanced growth inhibition to similar extents, irrespective of ring position. In contrast, analogues bearing 4-hydroxy or 4-acetamido groups (**1q** and **1r**, respectively) showed markedly reduced growth inhibition (IC_{50} >100 μ M). Biphenyl compounds **1s–1z** were then prepared to further investigate substituent effects at the 4-position. The most potent analogue was found to be the biphenyl-4-yl-containing compound (**1t**, IC_{50} = 0.7 μ M), which exhibited 100-fold greater antiproliferative potency than the unsubstituted parent **1a** (Table 1). The addition of electron donating or electron withdrawing groups (**1s** and **1v**, respectively) decreased antiproliferative potencies by from 4 to 6-fold. Introduction of *o*-methyl groups onto the biphenyl rings of **1t** resulted in greater than a 10-fold loss of potency (**1u**).

Although there appeared to be wide tolerance for structural diversity in the biphenyl series (**1s–1w**), the 4-phenoxyphenyl-containing analogue (**1w**) was distinct in showing a significant loss of toxicity (IC_{50} >100 μ M). This potentially indicated that geometric spacing of the two phenyl rings could be important for growth inhibition. That geometry could influence potency was also

Table 1
Growth inhibition of phenylmaleimides^a

No.	R ^b	IC ₅₀ (μ M)
1a		70
1b		9.0
1c		9.0
1d		7.0
1e		9.0
1f		9.0
1g		8.0
1h		9.0
1i		6.0
1j		6.0
1k		5.0
1l		9.0
1m		4.0
1n		7.0
1o		9.0
1p		10
1q		>100
1r		>100
1s		3.0

Table 1 (continued)

No.	R ^b	IC ₅₀ (μM)
1t		0.7
1u		10
1v		4
1w		>100
1x		3.5
1y		4.0
1z		1.8

^a Assays were run using HEP3B cells as described in the experimental procedures.

^b R group as indicated in Scheme 1.

Table 2
Growth inhibition of phenylalkylmaleimides^a

No.	R ^b	IC ₅₀ (μM)
2a		5.0
2b		2.5
2c		2.0
2d		1.0

^a Assays were run using HEP3B cells as described in the experimental procedures.

^b R group as indicated in Scheme 1.

supported by the fact that the growth inhibition of **1t**, which had a conformational minimum at a biphenyl torsional angle of 44°, is 10-fold lower than the bis-methyl-substituted biphenyl compound **1u**, where a conformational minimum exists when the phenyl rings are almost perpendicular to each other. In compounds **2a–2d** alkyl spacers were introduced between the maleimide nitrogen and the phenyl rings (Table 2). The growth inhibitory potencies of these analogues were similar to the 1- and 2-naphthyl systems (**1y** and **1x**) as well as the 2-anthracenyl system (**1z**) (Table 1). This indicated that conjugation through the aromatic system was not a critical determinant of antiproliferative potency.

The compounds in Tables 1 and 2 were designed to be Cdc25 phosphatase inhibitors that could theoretically function by 1,4-Michael-type alkylation of the catalytic cysteine thiolate anion. With an IC₅₀ value of 0.7 μM, the biphenyl-4-yl-containing maleimide **1t** was the most potent antiproliferative agent among the analogues examined. Therefore, crystallographic studies undertaken to obtain co-crystal structures of **1t** bound to Cdc25A protein. Cdc25A crystallizes readily and co-crystallization as well as crystal soaking

techniques were employed in efforts to obtain a structure of Cdc25A with bound inhibitor. In one protocol a molar excess of **1t** was incubated with the catalytic domain of Cdc25A and the solution was then set up for crystallization. Crystals appeared within 3–5 days and X-ray diffraction data were collected for numerous crystals up to a resolution of 2.0 Å. However, the electron density maps did not show any evidence of bound inhibitor. Rather, in many crystals electron density maps clearly revealed a disulfide linkage between the catalytic Cys430 residue and a proximal Cys384 residue.

Since co-crystallization studies failed to yield a structure with bound inhibitor, two strategies employing soaking methodologies were examined: In the first approach, crystals of the apo-form of Cdc25A were soaked with 1 mM **1t** in the presence of 5% v/v DMSO to enhance the solubility of the compound in the crystallization solution. Soaking times varied from 24 h to several days. Although the resulting crystals diffracted well, the electron densities did not show signs of bound inhibitor. In most cases, the active sites indicated the presence of the disulfide-linked cysteines. Based on the hypothesis that these disulfide linkages may prevent the covalent attachment of **1t** to the catalytic cysteine residue, crystals of Cdc25A were treated with the reducing agent tris-(2-carboxyethyl)phosphine (TCEP) immediately prior to soaking with **1t**. Although crystals from this experiment diffracted at up to 2.0 Å resolution, no inhibitor could be detected bound to the active site.

MALDI-TOF mass spectral studies were also undertaken to identify covalent adducts to Cdc25A protein following incubation with **1t**. A bromo-containing variant **1t** was also examined, since adducts could be easily identified by their 1:1 isotopic bromine doublets. Inhibitors were reacted with both wild-type Cdc25A and the C384A mutant. Incubation mixtures were subjected to tryptic digest prior to analysis by MALDI-TOF techniques. These experiments failed to detect peaks corresponding to covalent attachment of **1t** to the Cdc25A protein, indicating that the catalytic cysteine was not alkylated as expected.

In further work, a Cdc25A assay was set up using a 3-O-methyl fluorescein phosphate (OMFP) protocol. Although distinct enzyme inhibition could be shown for known naphthoquinone-based inhibitors (including **4**), which are hypothesized to function through a redox-mechanism, inhibition of Cdc25A by **1t** could not be shown. Furthermore, when aliquots of enzyme samples used in the mass spectrometry studies described above were assayed for inhibition by **1t** using a *para*-nitrophenyl phosphate assay, the wild-type enzyme and the two mutants did not show significant inhibition by **1t**. Finally, although Cdc25A is involved in the control of the G1/S transition,⁷ fluorescence activated cell sorting (FACS) analysis following treatment with **1t** showed that inhibition at one specific point in the cell cycle did not appear to occur as would be expected with inhibition of Cdc25A.^{8,9}

2.3. Activation of the unfolded protein response (UPR)

The endoplasmic reticulum (ER) is responsible for the synthesis of secretory, membrane and organelle-targeted proteins.¹⁰ Within the ER nascent polypeptide chains undergo necessary folding and post-translational modification, which includes the attachment of oligosaccharides and the formation of disulfide chains.¹¹ Certain cellular stresses, such as lowered pH values, reduced glucose levels, irradiation, the presence of reactive oxygen species (ROS) or genotoxic drugs, can adversely affect the ER's capacity to properly fold proteins, leading to activation of the UPR.¹² The UPR participates in cytoprotection through the temporary suspension of protein production, while at the same time upregulating ER chaperones that promote proper refolding. Under certain circumstances the UPR can facilitate induction of apoptosis.¹³

Although inhibition of Cdc25 phosphatases did not appear to be the cause of growth inhibition of the parent phenylmaleimide **1t**, transcriptional profiling of NEP3B cell in response to this compound identified a rapid increase in genes involved in the UPR, while leaving unchanged other stress inducible genes such as CDKN1A, DCD25A, CHEK1, BRCA1, MDM2 and GADD45B. Production of miss-folded or unfolded proteins causing endoplasmic reticulum (ER) stress and leading to UPR activation could potentially arise through alkylation of sulphhydryl groups on nascent polypeptide chains via 1,4-Michael-type addition onto the maleimide analogues. Such a mechanism is consistent with a report that the toxicity of arylating quinones is directly coupled to induction of

ER stress.¹⁴ The capability of phenylmaleimides to react as Michael acceptors with irreversible expulsion of one or both thioethanol groups was shown by reacting **1t** with *N*-acetylcysteine. Formation of the corresponding mono- and bis-cysteine adducts was shown by HPLC-MS.

In order to investigate whether the extent of UPR activation is related to growth inhibition by *N*-substituted maleimides, seven compounds (**1a**, **1r**, **1t**, **1w**, **1u**, **1v** and **2c**) from Tables 1 and 2 were selected for further examination. These analogues were re-evaluated for their antiproliferative potencies in HEP3B cells and in parallel examined at multiple concentrations (1, 10 and 50 μM) for their effects on the expression of five UPR-related genes (DDIT3, TRIB3, ATF4, GADD34, HSPA1A), which had been shown to be up-regulated following 1 h incubation with 10 μM of **1t**. These genes have been most closely allied with the UPR through protein kinase RNA (PKR)-like ER kinase (PERK) in response to ER stress.¹⁵ Another critical determinant of the UPR response, is the PERK-mediated phosphorylation at Ser51 of the 'Eukaryotic Translation Initiation Factor 2' on its alpha subunit (termed 'eIF2 α ').^{11,16}

The phosphorylation of eIF2 α was monitored concurrently with expression of the five UPR-related genes. Figure 2 shows dose-response curves that demonstrate the differential sensitivity of HEP3B cells to the seven selected analogues. These sensitivities ranged from the most potent analogue (**1t**) to the analog with no measurable activity in the assay (**1r**). Expression data after treatment with 2, 10 and 50 μM , of these analogues for 1 and 6 h, indicated that 10 μM incubation of each agent for 1 h allowed for a direct comparison of the magnitude of gene modulation. There were limited changes at 2 μM concentrations, while 50 μM concentrations were extremely toxic to the cells, making interpretation of comparative expression data difficult at these two concentrations.

Figure 3 identifies gene expression changes ($\pm\text{SD}$, $n = 3$) after 10 μM treatment with each analogue (1 h). ATF4, a member of the b-ZIP family of transcription factors,¹⁷ was induced approximately twofold in response to all the analogues to which the cells responded and it is one of the few genes that remains actively translated after the UPR response attenuates protein synthesis in response to ER stress.^{18,19} ATF-4 is responsible for transcriptional activation of a variety of UPR-responsive genes, including GADD34 (PP1R15A), which acts as a negative feedback loop to regulate

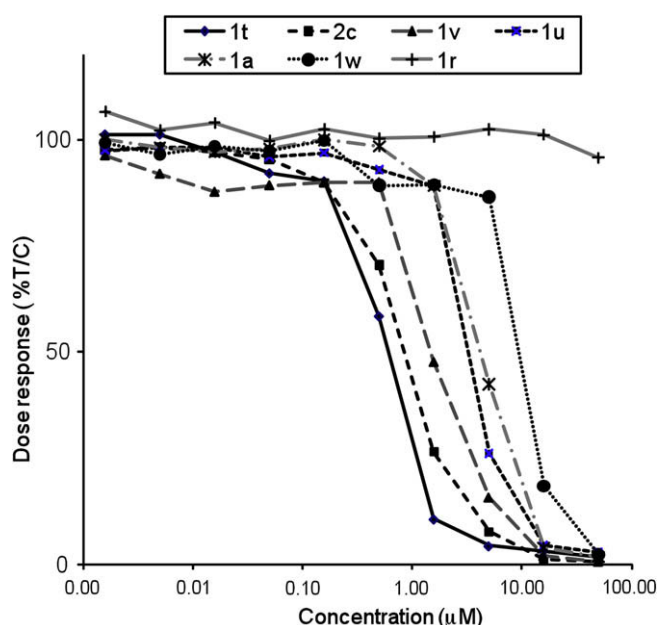


Figure 2. Sensitivity of HEP3B cell to indicated maleimide analogues. Cells were exposed to a range of analogue concentrations for 48 h, then survival was measured by the vital dye, alamar blue, and dose-response curves were calculated by (OD of treated/OD of control \times 100).

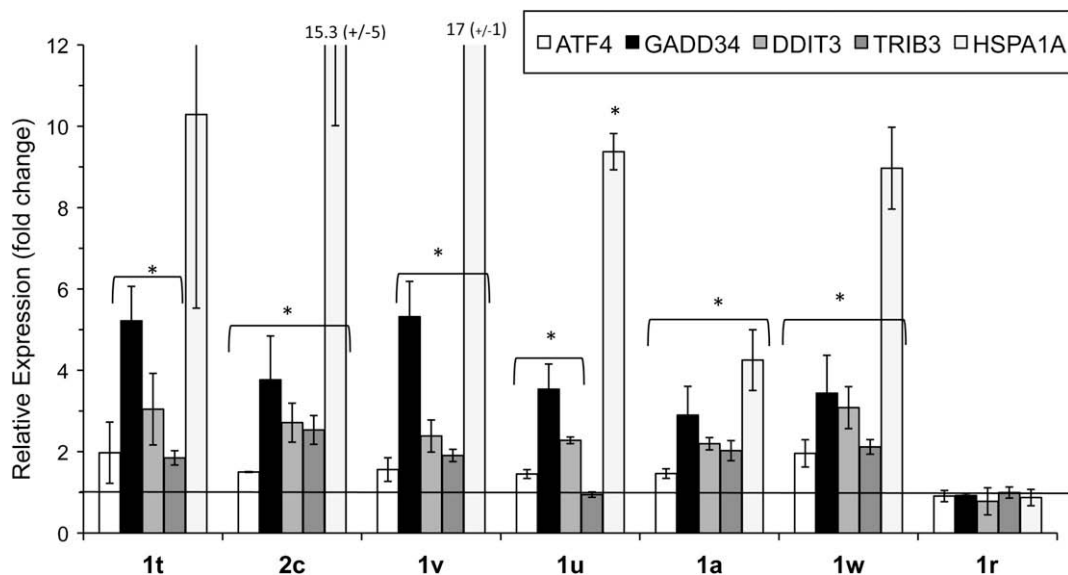


Figure 3. Induction of UPR-related gene expression after 1 h treatment with indicated analogs (10 μM). Genes were measured by real time PCR and expressed as fold change in treated cells compared to control cells ($n = 3 \pm \text{SD}$). * Represents situations where drug-induced gene expression is significantly different to control expression ($p < 0.05$).

eIF1 α phosphorylation,^{20,21} and provides an adaptive response to stress allowing protein synthesis to resume.²⁰ However, GADD34 over-expression has been demonstrated to elicit growth arrest and apoptosis^{22,23} in this study, the magnitude of induction of this gene was significantly correlated ($R = -0.824$, $p = 0.022$) with the potency of growth inhibition.

Another UPR-responsive transcriptional target of ATF-4, DDIT3 (CHOP/GADD153) was significantly up-regulated (~ 2 -fold) by all the active compounds. This has been identified as the most important gene responsible for induction of apoptosis when the UPR fails to resolve protein-folding defects.²⁴ The Tribbles 3 homolog (TRB3) has been identified as a target of CHOP/ATF4, and it is involved in CHOP-dependent cell death during ER stress.²⁵ TRB3 was transcriptionally activated by all the active analogues except **1u**. Finally, HSP1A1 was the most highly induced gene on the arrays. Although its activation is associated with generalized stress response, it has been linked to a pro-apoptotic role in ER stress.²⁶

Taken in total, the data convincingly indicates induction of a series of ER stress induced genes following treatment with the maleimides. This can be attributed to the UPR response induced by PERK activation of eIF2 α . Figure 4A demonstrates that there was a significantly greater activation of eIF2 α by phosphorylation

at Ser51 in HEP3B cells treated with the most potent analogs as compared to treatment with the less potent analogues. The extent of eIF2 α phosphorylation correlated significantly with HEP3B sensitivity to the analogues (Fig. 4B).

The results illustrate an essential paradox of stress response pathways, including the UPR, where response is designed to facilitate both stress adaptation as well as induction of apoptosis, depending upon the nature of the stress. Here we show that the ability of the maleimide analogues to induce UPR as measured by eIF2 α activation correlates highly with their antiproliferative potencies. This finding supports recent data indicating that bortezomib-induced apoptosis is directly related to its ability to maintain eIF2 α in a phosphorylated, active state.²⁷

3. Conclusion

Our current paper presents the synthesis and evaluation of maleimides that were designed to potentially serve as Cdc25 phosphatase inhibitors by alkylating catalytically-critical cysteine residues. In HepB3 cell culture assays, the analogues exhibited antiproliferative IC₅₀ values ranging from $>100 \mu\text{M}$ (e.g., **1q**, **1r**

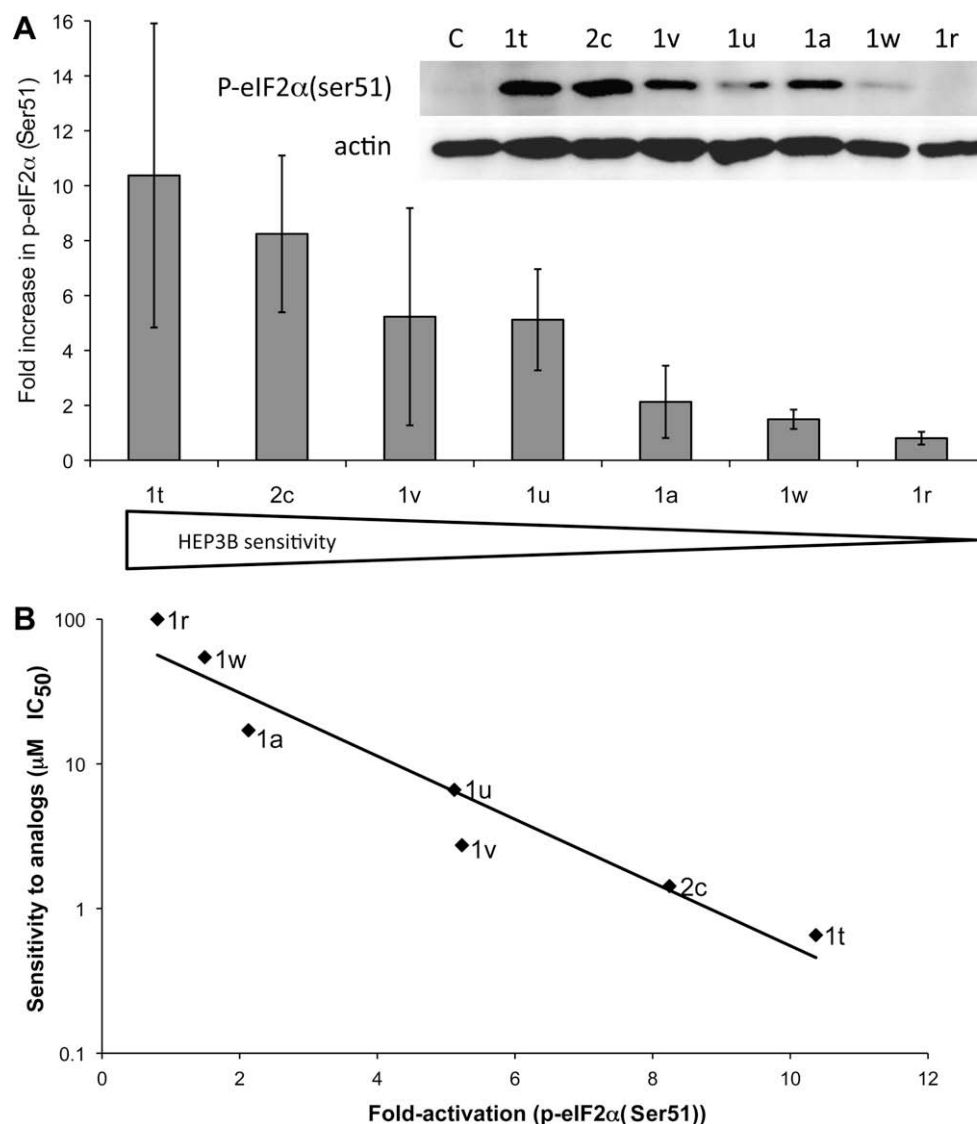


Figure 4. Correlation of activation of p-eIF2 α (Ser51) with HEP3B sensitivity (IC₅₀) to maleimide analogues. (A) A representative western blot of induction by analogues ordered by potency. The level of p-eIF2 α (Ser51) induction was calculated and graphed using normalization to actin expression ($n = 3 \pm \text{SD}$). (B) Linear regression curve for sensitivity and activation (average, $n = 3$) of eIF2 α $R = 0.964$, $p < 0.001$.

and **1w**) to sub-micromolar (**1t**). While the intended phosphatase inhibition through cysteine alkylation could not be demonstrated, studies with a subset of analogues correlated antiproliferative potencies with activation of the UPR response. These results may indicate the potential utility of UPR activation as means of achieving selective antiproliferative effects.

4. Experimental section

4.1. General

All chemicals used in syntheses were reagent grade (Aldrich, Milwaukee, WI) and were used without additional purification. Hexanes, ethyl acetate, methylene chloride, and methanol employed in chromatography were HPLC-grade. Flash chromatography was performed with Merck silica gel, 70–230 mesh and ISCO prepacked columns on a Teledyne ISCO CombiFlash Companion instrument. Analytical thin layer chromatography was performed on Analtech precoated plates (Uniplate, silica gel GHLF, 250 microns) containing a fluorescence indicator and compounds were visualized by UV and Hannesian agent (21 g of ammonium molybdate (VI) tetrahydrate, 1 g cerium sulfate tetrahydrate, 31 mL concentrated sulfuric acid, 469 mL H₂O) by warming with a heat gun. NMR spectra were recorded on Varian 200 or 400 MHz spectrometers with Me₄Si as an internal standard. Coupling constants are reported in Hertz, and chemical shifts are reported in the delta (ppm) scale; abbreviations s (singlet), d (doublet), t (triplet), q (quartet) and m (multiplet). Preparative HPLC was performed on a Beckman Coulter HPLC system equipped with 128P solvent module and 166P detector using a Phenomenex Jupiter C18 column (250 × 21.2 mm; particle size 4 μm). Solvent systems were H₂O/acetonitrile, 0.1% trifluoroacetic acid, gradient 5–100%. HPLC-MS analyses were performed on an Agilent 1100 Series LC/MSD model G1946A (Agilent Technologies Inc., Santa Clara, CA) with an API-electrospray source using a Zorbax 300SB-C18 Poroshell column (2.1 × 75 mm; particle size 5 μm) with a solvent system of H₂O/acetonitrile 0.5% acetic acid, gradient 5–100% over 4 min at a flow rate of 1 mL/min. High resolution mass spectra (HRMS) were acquired on an Agilent 6520 Accurate-Mass Q-TOF LC/MS System, (Agilent Technologies, Inc., Santa Clara, CA) equipped with a dual electro-spray source, operated in the positive-ion mode using a Zorbax 300SB-C3 Poroshell column (2.1 × 150 mm; particle size 5 μm). Data acquisition and analysis were performed using MassHunter software.

4.2. General procedure A: Preparation of 1-substituted-3,4-dibromomaleimides (**6a–6z**)

To a stirred solution of 3,4-dibromomaleic acid (**5**) in acetic acid on ice was added phenylamine (R-NH₂, [Scheme 1](#); 1.1 equiv) dropwise. The mixture was then stirred at reflux under argon (overnight). After cooling, the mixture was poured into ice water and extracted (ethyl acetate). The combined organic layers were washed with saturated sodium bicarbonate and brine and dried over magnesium sulfate. Removal of solvent provided crude product (**6a–6z**), which was purified by flash chromatography on silica gel (see [Supplementary data](#) for synthetic details and analytical data of individual compounds).

4.3. Procedure B: Preparation of 1-substituted-3,4-bis-(2-hydroxy-ethylsulfanyl)-maleimides (**1a–1z** and **2a–2d**)

To a solution of 3,4-dibromomaleimide (**6**) and imidazole (2.2 equiv) in THF was added 2-mercaptoethanol and the mixture was stirred (3 h). The reaction mixture was then partitioned between ammonium and ethyl acetate and the combined organic

layers were washed with brine and dried over magnesium sulfate. Removal of solvent gave crude product (**1a–1z** and **2a–2d**), which was purified by silica gel flash chromatography. All compounds were purified by HPLC chromatography (see [Supplementary data](#) for synthetic details and analytical data of individual compounds).

4.4. Growth inhibition assays

HEP3B cells (ATCC No. HB-8064) were purchased from the American Type Culture Collection (Rockville, MD). Cells were grown in Eagle's minimal essential medium (EMEM) supplemented with 10% heat-inactivated fetal bovine serum (FBS), 2 mmol/L L-glutamine, 100 units/mL penicillin and 100 μg/mL streptomycin. Cells were grown at 37 °C in humidified atmosphere consisting of 5% CO₂ and 95% air. Cells in exponential growth phase were used throughout. The sensitivity of HEP3B to seven selected maleimide analogs was tested following 48 h incubation with 1.6–50 μM of each analog. Growth inhibition (% treated/control) was calculated after a further 6 h incubation (37 °C) with the metabolic dye, alamar blue, (Sigma), and the fluorescence intensity measured on a Tecan Ultra plate reader (509-nm excitation and 520-nm excitation).

4.5. Transcriptional profiling

Human OperonV2, 20 K arrays, (National Cancer Institute microarray facility/Advanced Technology Center, Gaithersburg, Maryland) were utilized according to published protocols (www.nciarray.nci.nih.gov). Using competitive hybridization of treated versus untreated samples chemically coupled to a CyTM3 or CyTM5 fluorescently labeled dye (Amersham Biosciences, Little Chalfont Buckinghamshire, England), fluorescence was read on a GenePix 4100A microarray scanner (Axon Instruments, Union City, California). Data was analyzed using Axon GenePix Pro 4.1 software and data and image files were uploaded to the National Cancer Institute/Cancer Center for Research Microarray Center mAdB Gateway for analysis and comparison of multiple arrays.

4.6. Real time polymerase chain reaction assays

For each sample, five-hundred nanograms of total RNA was reverse transcribed using the High Capacity cDNA Reverse Transcription kit (ABI, Foster City, CA). Quantitative real time PCR reactions were conducted and measured using the ABI PrismTM 7500 Sequence Detection System and TaqMan[®] SYBR chemistries with primer pairs designed for each gene of interest. Samples were tested in triplicate wells for the genes of interest and for the endogenous control, GAPDH. Data was analyzed using the comparative Ct method as described in the Perkin Elmer User Bulletin #2 (ABI Prism[®] 7700 Sequence Detection System, 1997) and expressed as a fold induction of the gene in the drug treated samples compared to the untreated control samples.

4.7. Western blots

Whole cell protein lysates were prepared for protein analysis by western blot. Protein was quantitated using the Bradford Protein Assay (Bio-Rad Laboratories, Hercules, California), and approximately 50 μg of each sample was resolved using SDS-PAGE on 10% Tris glycine gels (Invitrogen, Carlsbad, California) and probed with phosphor-EIF2α (SER51) (Cell Signaling, Danvers, MA). Proteins were visualized using chemiluminescence and imaged using a KodakTM X-OMAT 2000A Processor (Rochester, New York).

Acknowledgments

We thank the staff of the Macromolecular Crystallography Laboratory Protein Production Core for preparing the Cdc25A protein

used in this study. This Work was supported in part by the Intramural Research Program of the NIH, Center for Cancer Research, NCI-Frederick and the National Cancer Institute, National Institutes of Health; in part by the Developmental Therapeutics Program in the Division of Cancer Treatment and Diagnosis of the National Cancer Institute; and in part with federal funds from the National Cancer Institute, National Institutes of Health, under contract N01-CO-12400. The content of this publication does not necessarily reflect the views or policies of the Department of Health and Human Services, nor does mention of trade names, commercial products, or organizations imply endorsement by the US Government.

Supplementary data

Supplementary data (synthetic details and compound physical data as well as experimental data showing 1,4 Michael-type addition of **1t** and *N*-acetyl cysteine presented) associated with this article can be found, in the online version, at [doi:10.1016/j.bmc.2010.04.057](https://doi.org/10.1016/j.bmc.2010.04.057).

References and notes

1. Kar, S.; Wang, M.; Yao, W.; Michejda, C. J.; Carr, B. I. *Mol. Cancer Ther.* **2006**, *5*, 1511.
2. Ham, S. W.; Park, H. J.; Lim, D. H. *Bioorg. Chem.* **1997**, *25*, 33.
3. Ham, S. W.; Park, J.; Lee, S. J.; Kim, W.; Kang, K.; Choi, K. H. *Bioorg. Med. Chem. Lett.* **1998**, *8*, 2507.
4. Nishikawa, Y.; Carr, B. I.; Wang, M.; Kar, S.; Finn, F.; Dowd, P.; Zheng, Z. B.; Kerns, J.; Naganathan, S. J. *Biol. Chem.* **1995**, *270*, 28304.
5. Kar, S.; Wang, M.; Ham, S. W.; Carr, B. I. *Biochem. Pharmacol.* **2006**, *72*, 1217.
6. Choi, D.-S.; Huang, S.; Huang, M.; Barnard, T. S.; Adams, R. D.; Seminario, J. M.; Tour, J. M. J. *Org. Chem.* **1998**, *63*, 2646.
7. Boutros, R.; Dozier, C.; Ducommun, B. *Curr. Opin. Cell Biol.* **2006**, *18*, 185.
8. Herzenberg, L. A.; Parks, D.; Sahaf, B.; Perez, O. D.; Roederer, M.; Herzenberg, L. A. *Clin. Chem.* **2002**, *48*, 1819.
9. Lyon, M. A.; Ducruet, A. P.; Wipf, P.; Lazo, J. S. *Nat. Rev. Drug Disc.* **2002**, *1*, 961.
10. Szegadi, E.; Logue, S. E.; Gorman, A. M.; Samali, A. *EMBO Rep.* **2006**, *7*, 880.
11. Malhotra, J. D.; Kaufman, R. J. *Antioxid. Redox Signal.* **2007**, *9*, 2277.
12. Schröder, M. *Cell. Mol. Life Sci.* **2008**, *65*, 862.
13. Rasheva, V. I.; Domingos, P. M. *Apoptosis* **2009**, *14*, 996.
14. Wang, X.; Thomas, B.; Sachdeva, R.; Arterburn, L.; Frye, L.; Hatcher, P. G.; Cornwell, D. G.; Ma, J. *Proc. Nat. Acad. Sci. U.S.A.* **2006**, *103*, 3604.
15. Ron, D.; Walter, P. *Nat. Rev. Mol. Cell Biol.* **2007**, *8*, 519.
16. Harding, H. P.; Zhang, Y.; Ron, D. *Nature* **1999**, *397*, 271.
17. Ma, Y.; Hendershot, L. M. J. *Biol. Chem.* **2003**, *278*, 34864.
18. Luo, S.; Baumeister, P.; Yang, S.; Abcouwer, S. F.; Lee, A. S. J. *Biol. Chem.* **2003**, *278*, 37375.
19. Zhang, K.; Kaufman, R. J. *Neurology* **2006**, *66*, S102.
20. Lee, Y. Y.; Cevallos, R. C.; Jan, E. J. *Biol. Chem.* **2009**, *284*, 6661.
21. Novoa, I.; Zeng, H.; Harding, H. P.; Ron, D. *J. Cell Biol.* **2001**, *153*, 1011.
22. Hollander, M. C.; Poola-Kella, S.; Fornace, A. J., Jr. *Oncogene* **2003**, *22*, 3827.
23. Yagi, A.; Hasegawa, Y.; Xiao, H.; Haneda, M.; Kojima, E.; Nishikimi, A.; Hasegawa, T.; Shimokata, K.; Isobe, K. *J. Cell. Biochem.* **2003**, *90*, 1242.
24. Malhotra, J. D.; Kaufman, R. J. *Semin. Cell Dev. Biol.* **2007**, *18*, 716.
25. Ohoka, N.; Yoshii, S.; Hattori, T.; Onozaki, K.; Hayashi, H. *EMBO J.* **2005**, *24*, 1243.
26. Kadara, H.; Lacroix, L.; Lotan, D.; Lotan, R. *Cancer Biol. Ther.* **2007**, *6*, 705.
27. Schewe, D. M.; Aguirre-Ghiso, J. A. *Cancer Res.* **2009**, *69*, 1545.